International Journal of Molecular Sciences

MDPI

Article

Compressive constraint promotes the cytotoxicity of PI3K signal targeted therapies in breast and pancreatic cancer cells

Di-Luoffo M.[1,2], Schmitter C.[1], Barrere E.C.[1], Therville N.[1], Chaouki M.[1], D'Angelo R.[1], Thibault B.[1], Delarue M.[1,2], Guillermet-Guibert J.[1,2*]

[1] Affiliation 1: Université de Toulouse, Inserm, CNRS, Université Toulouse III-Paul Sabatier, Centre de Recherches en Cancérologie de Toulouse, Toulouse, France ; Labex Toucan, Toulouse.
[2] Affiliation 2: - , CNRS, Toulouse, France.
* Correspondance: julie.guillermet@inserm.fr; Tel.: +33 5 82 74 16 52

Abstract (max 200 words):
Context: Mechanical stresses, including compressive stress, arise during cancer progression. The rapid tumor growth and massive extra-cellular matrix remodeling of breast and pancreatic cancers explain the high intensity of compressive constraint in those pathologies. However, the transduction of compressive constraint into biochemical signals in cancer cells and the sensitivity of compressed cancer cells to therapies that target those signals remains poorly known.
Results: We tested the effect of constant and high intensity 2D compression in four cancer cell lines where pharmacological and genetic PI3K inactivation alone decreased cell confluency. PI3K inhibition associated or not with compression accentuated cell confluency decrease and induced cell death, showing the importance of PI3K for cell survival under compression. Mechanistically, unbiased analysis identified that compression induced overexpression of PI3K isoforms and PI3K activation. Transcriptional effects of PI3K inhibition and compression converge to control mRNA and protein levels of an autophagy regulator GABARAP. PI3K inhibition and compression blocked autophagy, as assessed by accumulation of p62/SQSTM1 autophagosome cargo and decreased LC3B-II-mediated autophagy flux.
Conclusion: This study provides evidence for the role of PI3K in compression mechanotransduction. The balance between cell death and autophagy mediated by GABARAP level may sustain cell survival in compressive stress environment.

Citation: Lastname, F.; Lastname, F.; Lastname, F. Title. *Int. J. Mol. Sci.* **2021**, *22*, x. https://doi.org/10.3390/xxxxx

Academic Editor: Firstname Lastname

Received: date
Accepted: date
Published: date

Publisher's Note: MDPI stays

Keywords: PI3K-AKT, class I PI3Ks, compressive stress, mechanotransduction, autophagy, apoptosis, breast and pancreatic cancer cells.

neutral with regard to jurisdictional claims in published maps and institutional affiliations.

Copyright: © 2021 by the authors. Submitted for possible open access publication under the terms and conditions of the Creative Commons Attribution (CC BY) license (https://creativecommons.org/licenses/by/4.0/).

1. Introduction

In tissues, all cells are subjected to mechanical stresses, exerting a stress on the cell surface, which can be transmitted notably to the nucleus [1]. Physically, this stress is measured with internal tissue/cell resistance to deformation described in (N/m^2) or Pascal (Pa). Cells encounter three types of mechanical stresses: shear, tensile and compressive stress [2]. These mechanical interactions emerge from cell-cell or cell-substrate interaction [3]. Shear stress occurs when mechanical forces are applied parallel to a surface. Tensile and compressive stresses are perpendicularly directed, away and toward the cell surface, respectively. The impact of compressive stress on cell proliferation and migration depends on the magnitude, duration, and direction of applied forces, and is associated to extra-cellular tissue components [2]. At homeostasis, epithelial cells sense compressive forces that limit their proliferation [4]; hence, the values of compressive forces applied to epithelial cells remain low. During solid tumor development, tumor cells proliferate rapidly associated with an increase of intratumoral pressure [5]. The magnitude of pressure felt by tumor cells is of the order of hundred of Pa [5]. Rigidity of the stroma in which the tumor cells proliferate is increasing, promoting tumor cell confinement [6]. Those events lead to the emergence of large compressive stresses applied to confined tumor cells. *In vitro* 3D models of solid cancer cell growth under confinement show a cell proliferation decrease [7], while colon cancer cell compression without confinement promotes cancer cell growth [8]. Moreover, compression device can increase cancer cell invasive capabilities [9, 10]. Confinement increases their resistance to chemotherapeutic treatments; the latter is notably due to a maintained cell survival and reduced proliferation, limiting the effect of both cytotoxic/cytostatic agents [7, 11]. Currently, there is no way to predict what will be the cellular physiological response of compression or confinement in cancer cells.

Once exerted on a cell, a mechanical stress induces a mechanotransduction response, coupled to modification of gene expression, which is largely associated with Hippo pathway activation in response to tensile stress [12]. In tumors, Hippo pathway containing transcriptional regulators YAP/TAZ can reprogram cancer cells into cancer stem cells and incite tumor initiation, progression, and metastasis [12]. Further, the Hippo pathway crosstalks with morphogenetic signals, such as Wnt growth factors, and is also regulated by Rho and G protein-coupled receptor (GPCR), cAMP and PKA pathways [13]. In the last decade, research has highlighted the interconnections of signaling pathways, and other key intracellular signals involved in mechanotransduction were identified [14]. In this context, the pivotal role of phosphoinositide 3-kinases (PI3Ks) in mechanotransduction of cancers is emerging [15, 16]. However, PI3K pathway regulation under compressive stress response is not completely elucidated [14].

PI3K proteins can be divided into three classes (I–III) based on their primary structure, regulation, and *in vitro* lipid substrate specificity [17]. In the literature, the term PI3K refers usually to class I PI3K, which consists in one p110 catalytic subunit and one p85

regulatory subunit excepted for PI3Kγ which harbored a p55 regulatory subunit. This class, composed of four enzymes (α, β, δ, γ), with non-redundant functions [17, 18] and non-redundant roles in cancer [19], generates phosphatidylinositol 3,4,5-trisphosphate (PtdIns-3,4,5-P3 or PIP3) from phosphatidylinositol 4,5-bisphosphate (PtdIns-4,5-P2 or PIP2) [17]. This reaction is reversed by the phosphatase activity of Phosphatase and TENsin homolog (PTEN). In pancreatic cancer cells, compression-induced PI3K activation promotes migratory phenotype involving an autocrine auto-stimulation loop [9, 10, 20]. Class I PI3Ks are upstream activators of YAP/TAZ transcriptional pathway under tensile stress, positioning class I PI3Ks proteins as potential regulators of an essential mechanotransduction signaling [15]. In breast cancer cells, *in vivo* overexpression of PI3Kβ sensitizes untransformed cells to YAP/TAZ-induced oncogenicity [15]. Besides, PI3K/AKT signaling closely regulates autophagy process [21, 22]. Further, autophagy process was known to be induced by mechanical shearing and tensile stresses in cells, in physiological and especially in pathological conditions, further autophagy was involved in the integration of physical constraints [23-25]. Importantly, PI3K pathway is one of the most common aberrantly activated pathways in cancers. Genetic alterations of *PIK3CA* (gene encoding PI3Kα) or of *PTEN* lead to active PI3K signaling in breast cancer cells [26] and PI3K/AKT pathway is constitutively activated and associated with poor prognosis in pancreatic cancer [20]. Cancer dependency to PI3K activation of a wide range of solid cancers including breast and pancreatic cancers provided the rationale for development of inhibitors targeting PI3K/AKT pathway (reviewed in [27]) for their treatment.

While the role of tensile stress is now largely recognized as affecting tumor cell fate [28], the role of compressive stress is still emerging. In particular, the global cell signaling modification in response to compression remains poorly characterized. Recent evidence showed that, amongst all pro-tumoral signaling pathways, class I PI3Ks appear to be critically involved in the adaptive response to compression [9, 29] (reviewed in [14]). Hence, PI3K targeting small molecule inhibitors might be relevant therapies to annihilate this adaptive response and lead to cancer cell death. To test this hypothesis, we thus determined the importance of class I PI3K activity in cancer cell lines known to be sensitive to PI3K inhibitors and, using *in silico* transcriptome analysis, we identified GABARAP as a common molecular determinant associated with autophagy controlled by compression forces.

Here, our experimental and bioinformatics data brings new knowledge about PI3K/AKT pathway involvement in cell mechanotransduction under compression.

2. Results

2.1 PI3K pathway promotes cell confluency under compression in breast and pancreatic cancer cells

To experimentally investigate the involvement of PI3K in compression mechanotransduction, we treated with vehicle or a pan-PI3K inhibitor (GDC-0941 (10 μM)) breast (MCF-7 and MDA-MB-231) and pancreatic (PANC-1 and CAPAN-1) cancer

cell lines that were freely growing or growing with a 2D compression device using agarose pad with calibrated weight. The compressive constraints applied to each single cell were evaluated at 200 Pa (200 Pa) for 24h. We next quantified cell confluency after 0, 24h, 48h and 72h. All four cell lines harbored a significant decrease in cell confluency after GDC-0941 treatment or 200 Pa compression compared to uncompressed vehicle control condition (Figure 1A-D). The cell confluency of MCF-7 and CAPAN-1 significantly decreased by combining GDC-0941 and 200 Pa compression compared to GDC-0941 or 200 Pa conditions alone (Figure 1A-D); which was not observed in MDA-MB-231 and PANC-1 (Figure 1B, C). Compression or PI3K pharmacological inhibition decreases cell confluency of all cell lines; in two cell lines, pan-PI3K inhibitor further decreases cell confluency under 2D compression.

To further demonstrate the involvement of PI3K in mechanotransduction, we genetically decreased PI3Kα expression using shRNA gene silencing (sh PIK3α) in breast MCF-7 and MDA-MB-231 (Figure 2A) and pancreatic PANC-1 and CAPAN-1 (Figure 2B) cancer cell lines. Compared to scramble transduced cells (sh Scr), the genetic knockdown decreased at 45%, 68%, 38% and 44% the level of the p110α protein (catalytic subunit of PI3Kα) in MCF-7, MDA-MB-231 (Figure 2A) and PANC-1 and CAPAN-1 (Figure 2B), respectively. This genetic knockdown did not affect the level of other PI3K class I members such as PI3Kβ protein expression (Figure S1).

In addition to genetic knockdown, we applied 2D compressive constraints, with a single cell compression evaluated at 200 Pa (200 Pa); we quantified cell confluency after 0, 24h, 48h and 72h compression. All sh Scr and sh PI3Kα cell lines harbored a significant decrease in cell confluency under 200 Pa compression compared to uncompressed condition (Figure 2C-F). Additionally, the cell confluency of MCF-7 and CAPAN-1 significantly decreased by combining PI3Kα knockdown and 200 Pa compression compared to sh Scr or 200 Pa conditions alone (Figure 2C-F).

Thus all cell lines present a cell confluency decreased under either compression or PI3K inhibition. Besides, the MCF-7 and CAPAN-1 have a further compression-induced decrease in cell confluency with PI3K class I pharmacological inhibition or PI3Kα genetic knockdown under compression.

2.2 Compression and PI3K inhibitor increase apoptotic cell death in breast and pancreatic cancer cells

We next investigated by which mechanism cell confluency was decreased under PI3K pharmacological or genetic modulation. We performed Annexin V/Propidium Iodide (PI) cytometry experiments (Figure 3, S2). The basal cell death status was different depending on cell line. Interestingly 200 Pa compression increased total apoptosis in MCF-7, MDA-MB-231, PANC-1 and showed an increasing trend in CAPAN-1 cells (Figure 3, S2). Pan-PI3K inhibitor treatment (GDC-0941 (10 μM)) did not affect total apoptosis in all four cell lines. However, 200 Pa compression associated with pan-PI3K inhibitor treatment (GDC-0941 (10 μM, 24h)) increased total apoptosis although most importantly in MCF-7 and CAPAN-1 cells (Figure 3, S2).

In breast and pancreatic cancer cells, compression alone or associated with pan-PI3K inhibitor increase cell death; apoptosis status is modulated according to cell lines submitted to 200 Pa compression with or without PI3K inhibitor.

2.3 PI3K-AKT pathway-regulated gene expression is sensitive to compression in breast cancer cells

To go deeper in the molecular mechanism, we decided to analyze transcriptomic and to understand how compressive stress altered gene signature of cell signaling pathways, including PI3K pathway. To this end, we searched for datasets obtained upon compression of cancer cells in Gene Expression Omnibus database (GEO), where public sequencing data from published studies are available (Figure 4). In GEO database, one transcriptomic data obtained under cell compression is currently available. Kim *et al.* 2019 [30] compressed breast cancer cells and cancer associated fibroblasts (CAFs) using compressive pads applied on top of 2D cell layers. In this study, Kim *et al.* focused on and analyzed the action of compression on stromal cells. They observed that mechanical stress in these cells promoted a specific metabolic gene signature increasing glycolysis and lactate production [31]. Here, we compared the gene expression evolution of the two breast cancer cell lines MDA-MB-231 and MCF-7 that harbor decreased cell confluency under compression. Both breast cancer cell lines were compressed by a global compression applied on all cells ranging from 0 to 8kPa, and gene expression profile was analyzed. We first searched for gene signature enrichment analysis using canonical signatures from Gene Set Enrichment Analysis (GSEA) (Figure 4). The gene signatures in different pathways were normalized into transcripts per million and compared to housekeeping gene expression such as *ACTINB, LAMINA1* and *LAMIN* gene class. The expressions of these housekeeping genes were not affected by increasing compression (Figure S3A). Under increasing compression [0], [0.3-0.8], [1.5-4.0], [7.0-8.0] kPa, PI3K-AKT signature gene expression was significantly overexpressed in MDA-MB-231 cells, suggesting a global overexpression of genes belonging to these pathways, while it was found already high in MCF-7 cells (Figure S3B, left panel). Those results are pertinent with known genetic status of MCF-7 cells, in which PI3Kα is constitutively active by mutation of its encoding gene (*PIK3CA*^{E545K}). However, *PIK3CA*, *PIK3CB* and *PIK3CD* expressions increased in MCF-7 cells and remained stable in MDA-MB-231 cell line (Figure S3B, right panel).

Interestingly, YAP/TAZ pathway gene signature was not significantly affected by increasing compression in both MCF-7 and MDA-MB-231 cells (Figure S3C, left panel). These transcriptomic results were experimentally confirmed by RT-qPCR analyzing gene expression of YAP/TAZ pathway members such as *TEAD1* and *c-JUN* and of downstream effectors of YAP/TAZ pathway such as *CCN1* and *CCN2*. The expression level of those genes were not significantly modulated when we applied a 200 Pa/cell 2D compression (200 Pa) using agarose pad with calibrated weight in breast cancer cells (MCF-7 and MDA-MB-231) (Figure S4A) as well as in pancreatic cancer cells (PANC-1 and CAPAN-1) (Figure S4B). We observed however a modest (1.36-fold) increase expression of *CCN2* in MCF-7 cells (Figure S4A). Those transcriptomics data were confirmed by other molecular assays such as the study of YAP phosphorylation that control its nuclear

translocation. The p-YAP^{S127}/YAP ratio was not significantly changed under 200 Pa compression in pancreatic and breast cancer cell lines (Figure S4C).

Taken together, these data showed an increased gene expression of PI3K family members in cells growing under compression (from 0 to 8 kPa) in MCF-7 cells.

2.4 Compression activates PI3K pathway gene expression in breast and pancreatic cancer cells

To validate experimentally the compression impact on PI3Ks expression, we next compressed breast and pancreatic cells and analyzed gene expression of 6 PI3K-AKT pathway genes including the four class I PI3K genes (*PIK3CA*, *PIK3CB*, *PIK3CD* and *PIK3CG*), *PTEN* and *EIF4A*. mRNA level analysis revealed respectively a 2.9-fold and 6.2-fold overexpression of *PIK3CA* and *PIK3CD* genes in MCF-7 cells. There was also a 3.5 and 2.4-fold increase of *EIF4E* gene expression in MCF-7 and MDA-MB-231 cells respectively (Figure 5A). Moreover, at protein level, compression significantly increased by 3.5-fold p-AKT^{S473}/total AKT ratio, indicative of PI3K activation in MCF-7 (Figure 5C). In PDAC cancer model, cells harbored a 11.7-fold significant *PIK3CG* overexpression in PANC-1 and a 2.7-fold, 4.9-fold significant overexpression of *PIK3CB* and *PIK3CG* respectively in CAPAN-1 (Figure 5B). Further, *PIK3CB* gene expression was also increased, 8.1-fold (p-value=0.07) and 2.7-fold (p-value=0.04) under 200 Pa compression in PANC-1 and CAPAN-1 cells respectively (Figure 5B). Finally, p-AKT^{S473}/total AKT ratio is constitutively high and maintained high under compression in PANC-1 cells and further compression significantly increased by 2.9-fold p-AKT^{S473}/total AKT ratio in CAPAN-1 (Figure 5D).

These experimental results show in 3 of 4 cell lines the mRNA overexpression of important PI3K pathway members, that are class I PI3K genes (*PIK3CA*, *PIK3CB*, *PIK3CD*, *PIK3CG*). The activation of PI3K pathway as assessed by AKT phosphorylation under 2D compression is mostly increased in MCF-7 and CAPAN-1 cancer cells, and maintained at high level in PANC-1 cells.

2.5 PI3K pathway-regulated and compression-regulated gene expression share common targets and control autophagy gene expression in breast cancer cells

To investigate the specific role of PI3K isoforms in the response to compression, we analyzed data from two more studies, which used selective inhibitors of PI3K isoforms: Bosch *et al.*, 2015 [32] and Lynch *et al.*, 2017 [33]. The authors used BYL719 or AZD8186 compounds described as selective inhibitors of PI3Kα or PI3Kβ respectively, in mutant *PIK3CA* MCF-7 and mutant *PTEN* HCC70 breast cancer cells. Mutant *PTEN* leads to increased PI3K activity [34]. We next used gene expression data from PI3Kα inhibition in MCF-7 and PI3Kβ inhibition in HCC70 cells to define PI3Kα and PI3Kβ signatures. Selective transcriptional targets were crossed-compared with the compression-specific transcriptional targets that we previously identified (Figure 4).

After PI3Kα inhibition in MCF-7, 1279 genes had a significantly altered expression. After PI3Kβ inhibition in HCC70 cells, gene expression of 933 genes was also significantly affected. Gene expression of 1052 targets was affected in compressive conditions ([0.3-0.8], [1.5-4.0] and [7.0-8.0] kPa compared to [0] kPa) in MCF-7 cells. We compared these sig-

natures to the list of the 102 genes found in canonical "PI3K-AKT REACTOME signaling pathway in cancer" signature (Figure 6). PI3Kα and PI3Kβ signatures overlapped with the regulation of 139 genes (listed in Figure 5, top table). Compressive stress gene signature mostly overlapped either with PI3Kα or PI3Kβ signatures, on non-common 32 and 31 genes respectively (listed in Figure 5, left and right tables respectively), suggesting a differential effect on isoform activation in response to compression.

Finally, GABA type A receptor associated protein like 1 gene (*GABARAPL1)*, coding for GABARAP structural protein of the autophagosome, was the only common target gene differentially expressed between PI3Kα signature, PI3Kβ signature, compressive stress signature and "PI3K-AKT REACTOME signaling pathway in cancer" signature (Figure 6). *GABARAPL1* and autophagy GSEA pathway gene signatures were affected under increasing compression in breast cancer cells (Figure 6, lower panel). In details, *GABARAPL1* gene expression was significantly upregulated after PI3Kα (x1.90; p-value=0.08) and PI3Kβ (x1.42; p-value=0.006) inhibitions. Under increasing compression from [0] kPa up to [7.0-8.0] kPa, *GABARAPL1* gene expression was increased in MDA-MB-231 cells, but not in MCF-7 cells (Figures 6-7), suggesting an association between PI3K activation and GABARAPL1 expression under compression. Moreover, under increasing compression, the canonical autophagy GSEA pathway gene expression significantly increased in MDA-MB-231 cells and decreased in constitutive PI3K activated MCF-7 cells (Figure S3C, right panel).

These analyses show that compression and PI3K signaling share common transcriptional targets, and that PI3Kα and PI3Kβ gene signatures are altered upon compression; those gene expression alterations converge towards the regulation of autophagosome structural genes.

2.6 Compression modulates the expression of autophagosome structure proteins in breast and pancreatic cancer cells

Autophagy process was proposed as a therapeutic target for various tumors [21]; inhibition of autophagy in cancer cells decreases their survival. PI3Kα and PI3Kβ are known to be positive and negative regulators of autophagy process [21, 22]. When comparing PI3Kα and PI3Kβ signatures, PI3K-AKT REACTOME canonical pathway and compressive stress selective gene expression, only *GABARAPL1* gene was significantly affected and overlapped in these four signatures (Figure 6). Briefly, this gene encodes for a structural protein of the autophagosome and autophagolysosome involved in autophagy process (reviewed in [35]). To validate transcriptomics data, we decided to analyze autophagy genes as well as *GABARAPL1* gene expressions in compressed cells. In MDA-MB-231 cells, no significant modulation of *ATG12*, *ATG4A*, *ATG14*, *PIK3C3*, *PIK3R4* gene expressions was measured (Figure 7A, right panel). However, a heterogeneous response for *ATG12*, *ATG14*, *PIK3C3*, *PIK3R4* gene expressions in MCF-7 cells, under compression for 24h was observed (Figure 7A, left panel). In agreement with transcriptomic data analysis (Figure 6, lower panel), *GABARAPL1* gene expression was significantly increased by 2.1-fold (p-value=0.01) in MDA-MB-231 (Figure 7A, right panel)

and not affected in MCF-7 (p-value=0.36) (Figure 7A, left panel). Next, the GABARAP protein level was analyzed. According to gene expression, the 200 Pa compression significantly increased by 5.9-fold GABARAP protein level (p-value=0.04) in MDA-MB-231 and no difference was measured in MCF-7 compared to control (0 Pa) (Figure 7C). We expanded our analysis to pancreatic cancer cells. PANC-1 cells harbored an increasing trend for *ATG14* gene expression (Figure 7B, left panel, p-value=0.06) However, CAPAN-1 cells showed no significant modulation of *ATG12*, *ATG4A*, *ATG14*, *PIK3C3* and *PIK3R4* gene expressions (Figure 7B, right panel) under 200 Pa for 24h. For *GABARAPL1* gene expression, only PANC-1 cells harbored a 3.0-fold *GABARAPL1* gene overexpression under 200 Pa compression for 24h (Figure 7B). GABARAP protein level was significantly decreased (0.47-fold; (p-value=0.003)) in CAPAN-1 cells and not affected in PANC-1 cells (Figure 7D). The basal level of GABARAP was found higher in PANC-1 cells compared to all other cell lines.

These experimental results confirmed the transcriptomics data and showed no significant autophagy gene modulation at single gene level under 2D compression in the four cell lines tested. However, *GABARAPL1* gene expression is increased in MDA-MB-231 mammary cells and PANC-1 pancreatic cells; the GABARAP protein is increased in MDA-MB-231 and high in PANC-1 cells. Reversely, GABARAP protein expression is low in MCF-7 and decreased in CAPAN-1 cells. Interestingly, those cells lines are the ones in which compression further activates PI3K signaling suggesting a potential crosstalk of compression and PI3K activation in controlling autophagy depending on the breast or pancreatic cell line.

2.8 Pharmaceutical inhibition of PI3K decrease the autophagy flux in breast and pancreatic cancer cells

Then, we decided to investigate the cellular localization of the autophagosome cargo p62/SQSTM1 by immunofluorescence. Its accumulation in puncta is usually observed when autophagy process is blocked [36]. We observed the p62/SQSTM1 level and localization in breast and pancreatic cancer cells under compression. A 200 Pa compression increased the density and the perinuclear localization of p62/SQSTM1 puncta in four cell lines.

We next wondered whether PI3K inactivation in MCF-7 and CAPAN-1 might be able to further block autophagy process under compression and quantified the level of autophagy flux. At autophagosome initiation, LC3B-I is lipidated in LC3B-II [21, 22]. Next, LC3B-II autophagosomes are degraded by fusion with lysosomes. To assess the level of LC3B-II-autophagic flux, we used chloroquine (10 μM) that inhibits autophagy by impairing autophagosome fusion with lysosomes [37], to determine the amount of LC3B-II-autophagosomes that is at this time point degraded by lysosomes. Comparing LC3B-II level of chloroquine-treated to controls in the different conditions is thus a mean to assess changes in LC3B-II-mediated autophagy flux.

In all cancer cell lines (Figure 8B-E), in absence of compression, the LC3B-II-autophagy flux was decreased upon PI3K inhibitor treatment, as treating the four cancer cell lines

with pan-PI3K inhibitor (GDC-0941 (10 μM)) increased basal LC3B-II level but did not significantly further increased LC3B-II levels under chloroquine. PI3K activity promoted autophagy flux. Compression drastically reduced LC3B-II-autophagy flux, as compression did not lead to accumulation of LC3B-II and the level of LC3B-II under chloroquine was significantly reduced compared to uncompressed condition (Figure 8B-E). However, the LC3BII-autophagy flux under compression appeared as increased by PI3K inhibition (Figure 8B-E); this was particularly significant in CAPAN-1 cells (Figure 8E). While compression blocks autophagy, PI3K activation maintains autophagy in compressed cancer cells.

Figures, Tables and Schemes

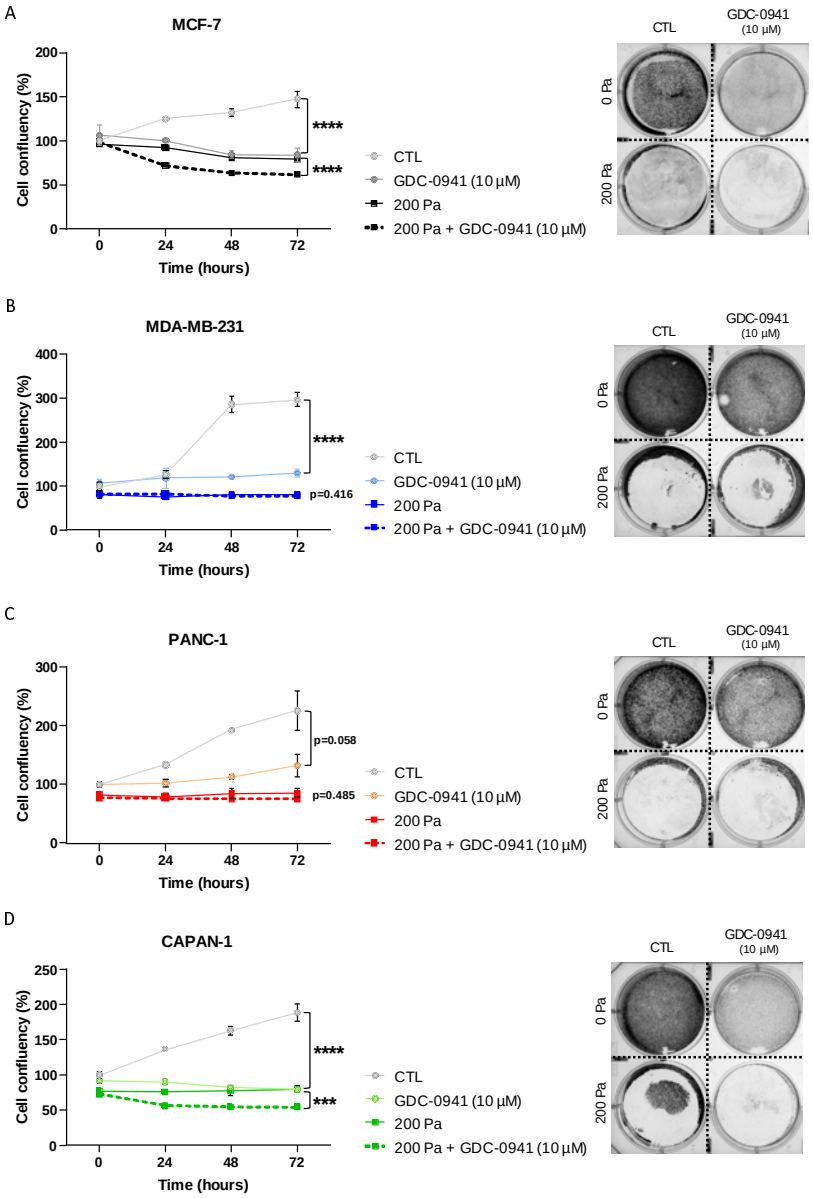

Figure 1. Cell confluency in MCF-7/MDA-MB-231 breast and PANC-1/CAPAN-1 pancreatic cancer cells after pharmaceutical inhibition of class I PI3K and 200 Pa compression. After cell treatment and/or compression, cell confluency was quantified using Crystal Violet staining (**A-D**, left). Pictures of representative experiments performed in 6-well plates after 72h are shown (**A-D**, right). Cell confluency was analyzed at 0, 24, 48 and 72 hours in MCF-7, MDA-MB-231, PANC-1 and CAPAN-1 cells were treated with pan-PI3K inhibitor (GDC-0941 (10µM)), 200 Pa compressed or with pan-PI3K inhibitor (GDC-0941 (10µM)) and 200 Pa compressed (dotted curves) compared to control cells. Quantitative analyses were performed using ImageJ software. Results are presented as mean, +/- SEM, n=3. p=p-value after two-way ANOVA; ***p-value<0.0004; ****p-value<0.0001.

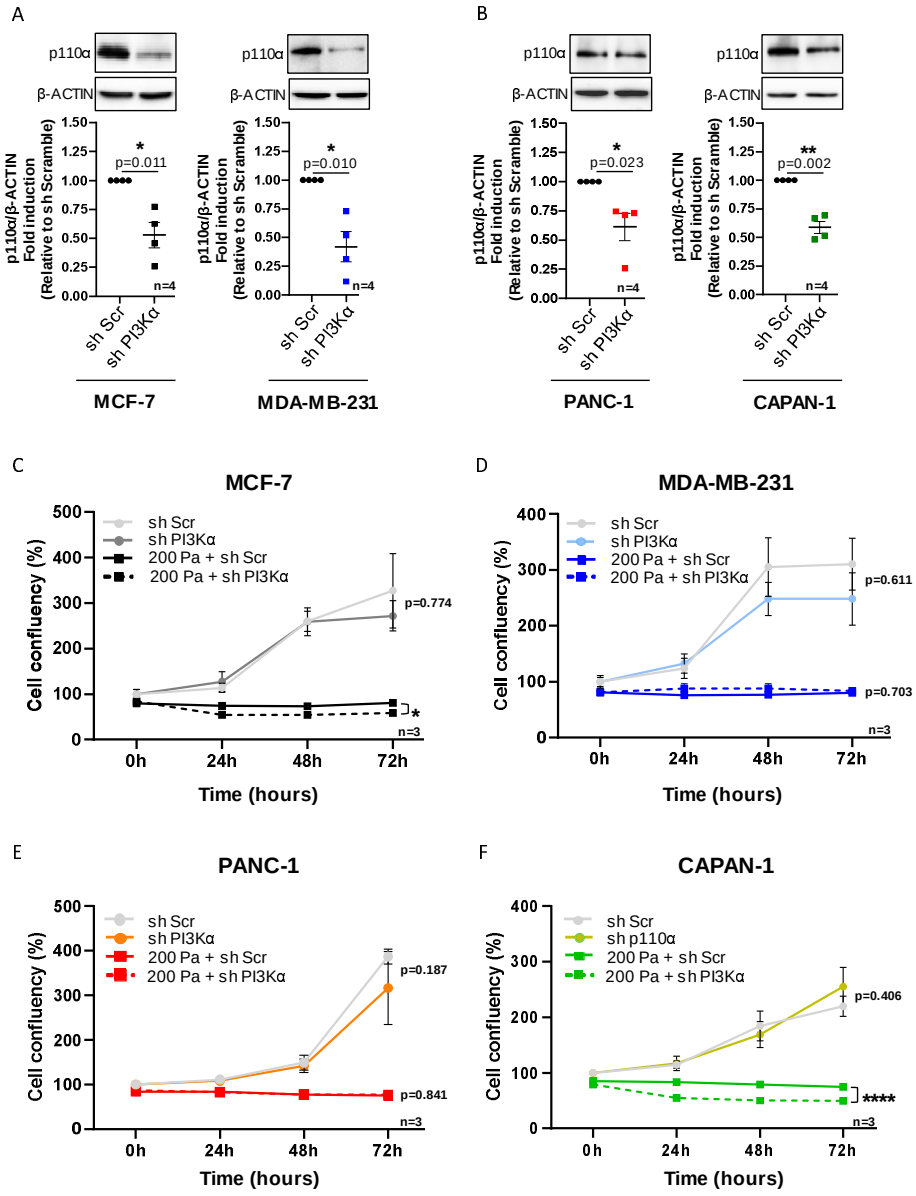

Figure 2. Cell confluency in MCF-7/MDA-MB-231 breast and PANC-1/CAPAN-1 pancreatic cancer cells after genetic knockdown of PI3Kα under 200 Pa compression. Representative western blots of p110α in MCF-7/MDA-MB-231 (**A**) and in PANC-1/CAPAN-1 (**B**) cells after genetic knockdown of PI3Kα (sh PI3Kα) *versus* sh scramble (sh Scr). β-ACTIN was used as loading control. Quantitative analyses were performed using ImageJ software. Results are presented as mean, +/- SEM, n=4. *p-value<0.05, **p-value<0.005. **C-F**. Cell confluency was analyzed at 0, 24, 48 and 72 hours in MCF-7, MDA-MB-231, PANC-1 and CAPAN-1 cells after PI3Kα genetic knockdown (sh p110α), 200 Pa compressed or after PI3Kα genetic knockdown (sh p110α) and 200 Pa compressed (dotted curves) compared to control cells. Quantitative analyses were performed using ImageJ software. Results are presented as mean, +/- SEM, n=3. p=p-value after two-way ANOVA; *p-value<0.05; ****p-value<0.0001.

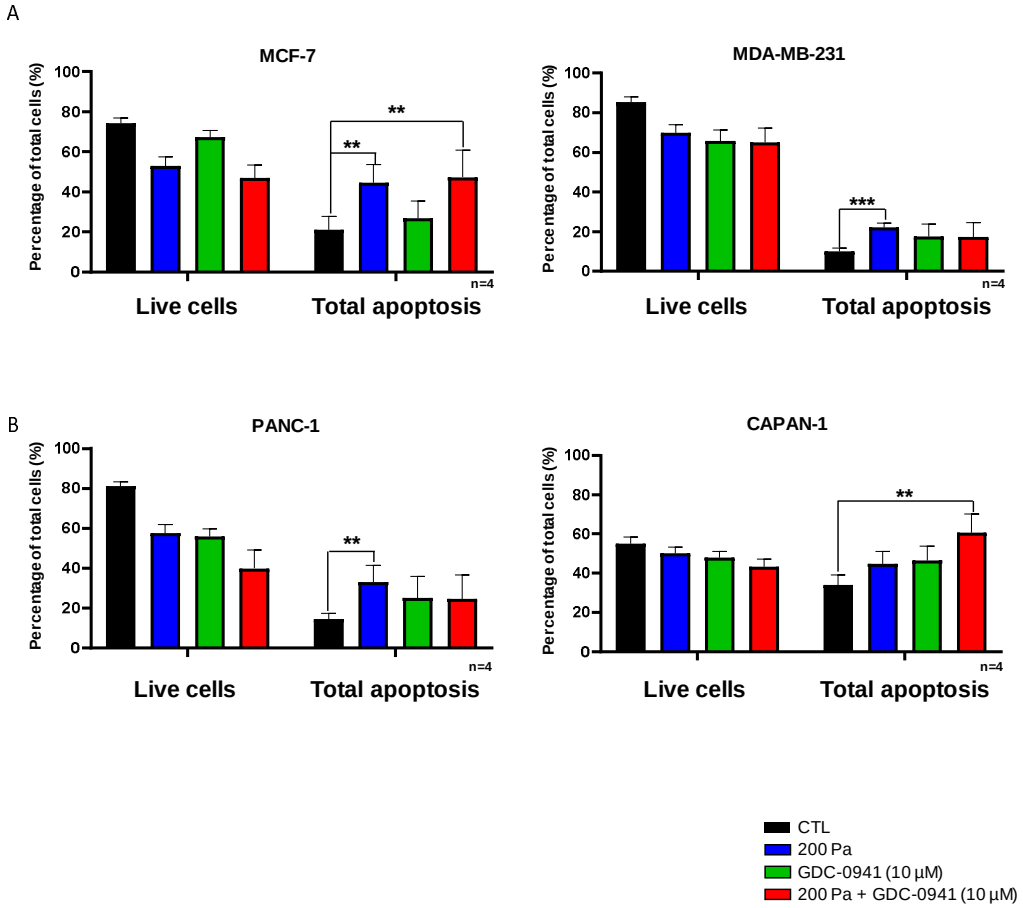

Figure 3. *In vitro* induction of total apoptosis in MCF-7/MDA-MB-231 breast and PANC-1/CAPAN-1 pancreatic cancer cells after pharmaceutical inhibition of class I PI3K and 200 Pa compression. After 24h pan-PI3K inhibitor treatment and/or compression, cells were stained with a FITC-Annexin V/PI apoptosis detection kit. FITC-Annexin staining and Propidium Iodide (PI) incorporation were measured in cells using a flow cytometer and analyzed using FlowJo software. Apoptotic cell populations were measured in MCF-7 (**A**), MDA-MB-231 (**B**), PANC-1 (**C**) and CAPAN-1 (**D**) cells in control (CTL, black bar), 200 Pa compressed (200 Pa, blue

bar), pan-PI3K inhibitor (GDC-0941 (10μM), green bar) and 200 Pa compressed with pan-PI3K inhibitor (200 Pa + GDC-0941 (10μM), red bar) conditions. Total apoptosis corresponds to the addition of Early and Late apoptosis in Figure S2. Results are presented as mean, +/- SEM, n=4. p=p-value after two-way ANOVA; **p-value<0.005; ***p-value<0.001.

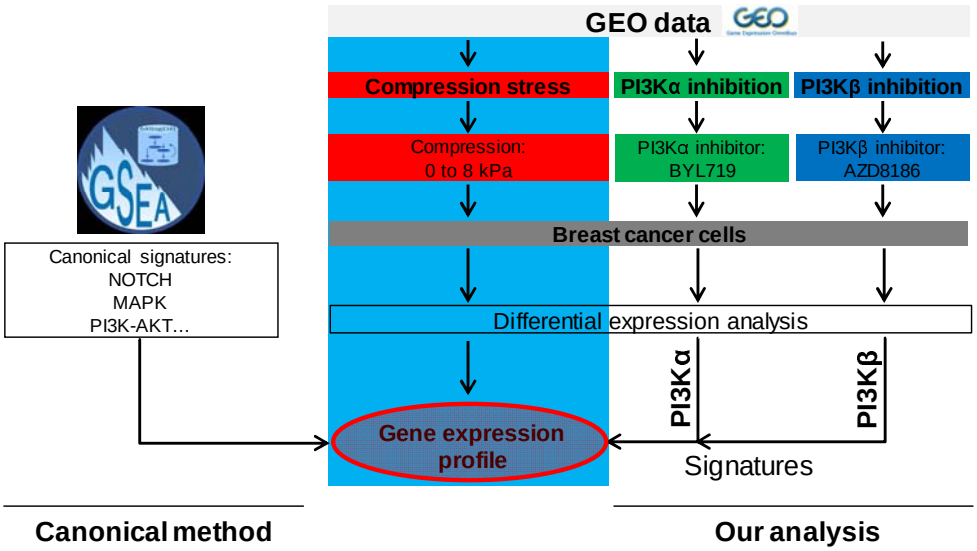

Figure 4. **PI3K-AKT: a pathway involved in mechanotransduction in breast cancer cells**. Available transcriptomic data from compressed breast cancer cells were downloaded from Gene Expression Omnibus data (GEO) from Kim *et al.*, 2019: https://www.ncbi.nlm.nih.gov/geo/query/acc.cgi?acc=GSE133134. Breast cancer cells (MDA-MB-231: $PIK3CA^{wt}$ and MCF-7: ($PIK3CA^{E545K}$ mutated) were compressed from 0 to 8 kPa and then a differential expression analysis was performed between 0; [0.3 to 0.8 kPa]; [1.5 to 4.0 kPa]; [7.0 to 8.0 kPa] respectively. On the left side, the canonical analysis method consisting in Gene Set Enrichment Analysis (GSEA) using commonly used canonical signatures. In parallel, differential expression analysis was performed from breast cancer cells treated with two PI3K inhibitors (PI3Kα (BYL719) and β (AZD8186)) (Bosch *et al.*, 2015 and Lynch *et al.*, 2017). The gene expression profiles after PI3Kα and β inhibitions (PI3Kα and β signatures) were compared to that obtained in the compressive stress study.

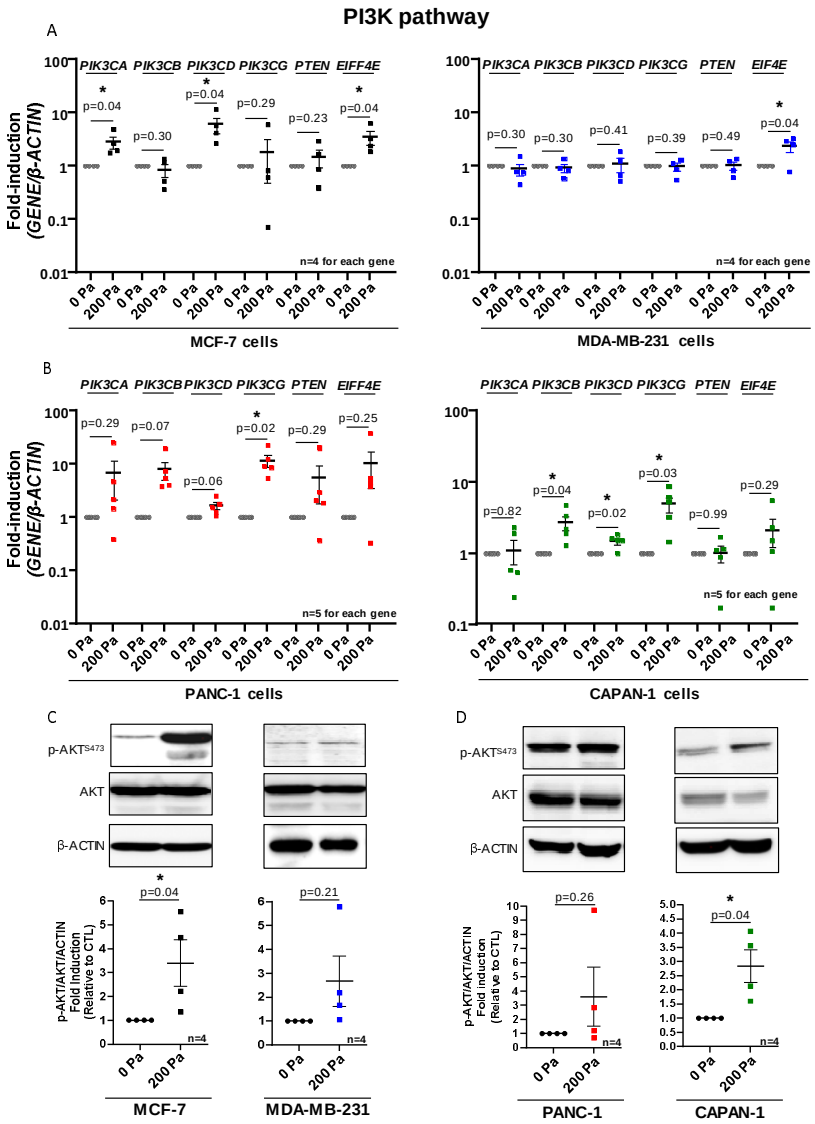

Figure 5. **PI3K signaling in breast and pancreatic cancer cells under 200 Pa compression**.

A,B. Representation of *PIK3CA*, *PIK3CB*, *PIK3CD*, *PIK3CG*, *PTEN* and *EIF4E* mRNA expressions in MCF-7 (A, left panel), MDA-MB-231 (A, right panel), PANC-1 (B, left panel) and CAPAN-1 (B, right panel) cells compressed at 200 Pa/cell range value in 2D (200 Pa) compared to non-compressed cells (0 Pa) for 24h. β-ACTIN was used as housekeeping gene. Results are presented as mean, +/- SEM. n≥4 for each gene. **C,D**. Representative western blots of p-AKT^{S473} and AKT in MCF-7/MDA-MB-231 and in PANC-1/CAPAN-1 cells under 200 Pa compression (200 Pa) and non-compressed cells (0 Pa) for 24h. β-ACTIN was used as loading control. p-AKT^{S473}/AKT quantitative analyses were performed using ImageJ software. Results are presented as mean, +/- SEM, n=4. *p-value<0.05.

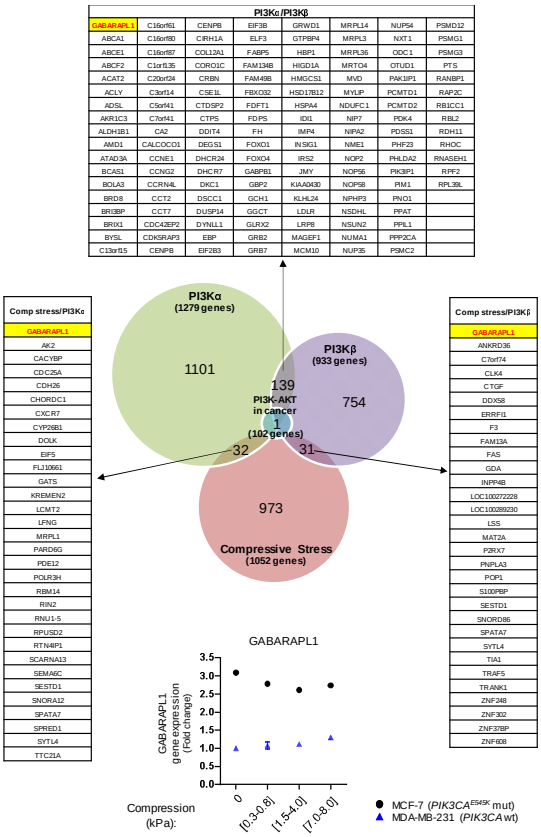

Figure 6. **Comparative analysis between compressive stress, PI3Kα/PI3Kβ and PI3K-AKT signaling in cancer gene signatures**. The lists of 1279, 933 and 1052 differentially expressed genes in PI3Kα signature, PI3Kβ signature, compressive stress signature and 102 genes of REACTOME PI3K-AKT signaling in cancer signature were compared. Venn diagram shows the overlapping between PI3Kα signature, PI3Kβ signature, compressive stress and REACTOME PI3K-AKT signaling in cancer. Tables represent the overlapping between compressive stress/PI3Kα signature (32 genes) (bottom left), compressive stress/PI3Kβ signature (31 genes) (bottom right) and PI3Kα/PI3Kβ signatures (139 genes) (above center). The only common gene differentially expressed in PI3Kα inhibition/PI3Kβinhibition/compressive stress was *GABARAPL1* (highlighted in yellow). MDA-MB-231 (*PIK3CA*^{wt}; blue triangles) and MCF-7 (PIK3CA^{E545K} mutated, black dots) breast cancer cells were gradually compressed (0 kPa; [0.3 to 0.8 kPa]; [1.5 to 4.0 kPa]; [7.0 to 8.0 kPa] respectively) and *GABARAPL1* gene expression was quantified using Agilent microarray (Data available in https://www.ncbi.nlm.nih.gov/geo/query/acc.cgi?acc=GSE133134).

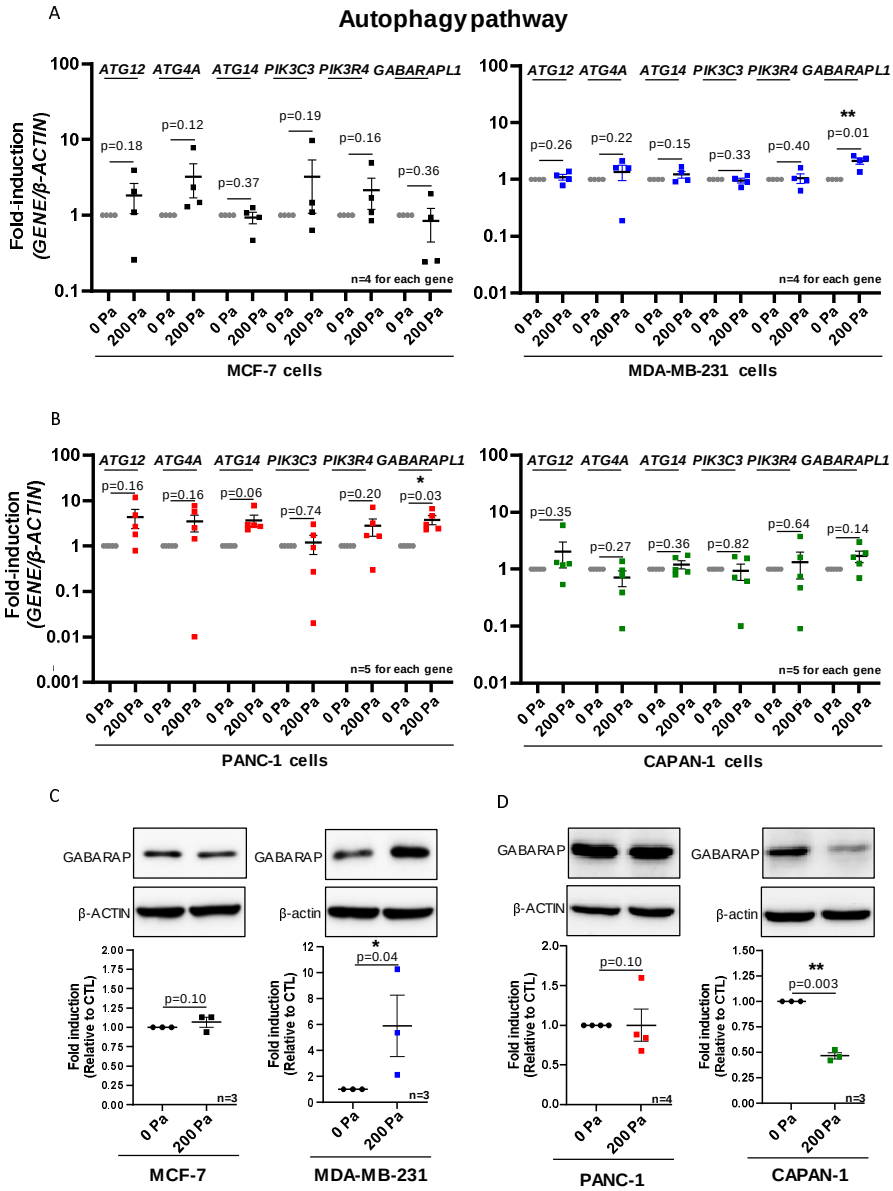

Figure 7. **Autophagy pathway in MCF-7/MDA-MB-231 breast and PANC-1/CAPAN-1 pancreatic cancer cells under 200 Pa compression**. **A,B**. Representation of *ATG12*, *ATG4A*, *ATG14*, *PIK3C3*, *PIK3R4* and *GABARAPL1* mRNA expressions in MCF-7 (A, left panel) and MDA-MB-231 (A, right panel) and in PANC-1 (B, left panel) and CAPAN-1 (B, right panel) cells 200 Pa compressed (200 Pa) compared to non-compressed cells (0 Pa) for 24h. β-ACTIN was used as housekeeping gene. Results are presented as mean, +/- SEM. n≥4 for each gene. **C,D**. Representative western blots of GABARAP in MCF-7 and MDA-MB-231 (C) and in PANC-1 and CAPAN-1 cells (D), 200 Pa compressed (200 Pa) and non-compressed cells (0 Pa) for 24h. β-ACTIN was used as loading control. GABARAP/β-ACTIN quantitative analyses were performed using ImageJ software. Results are presented as mean, +/- SEM, n≥3. *p-value<0.05; **p-value<0.01.

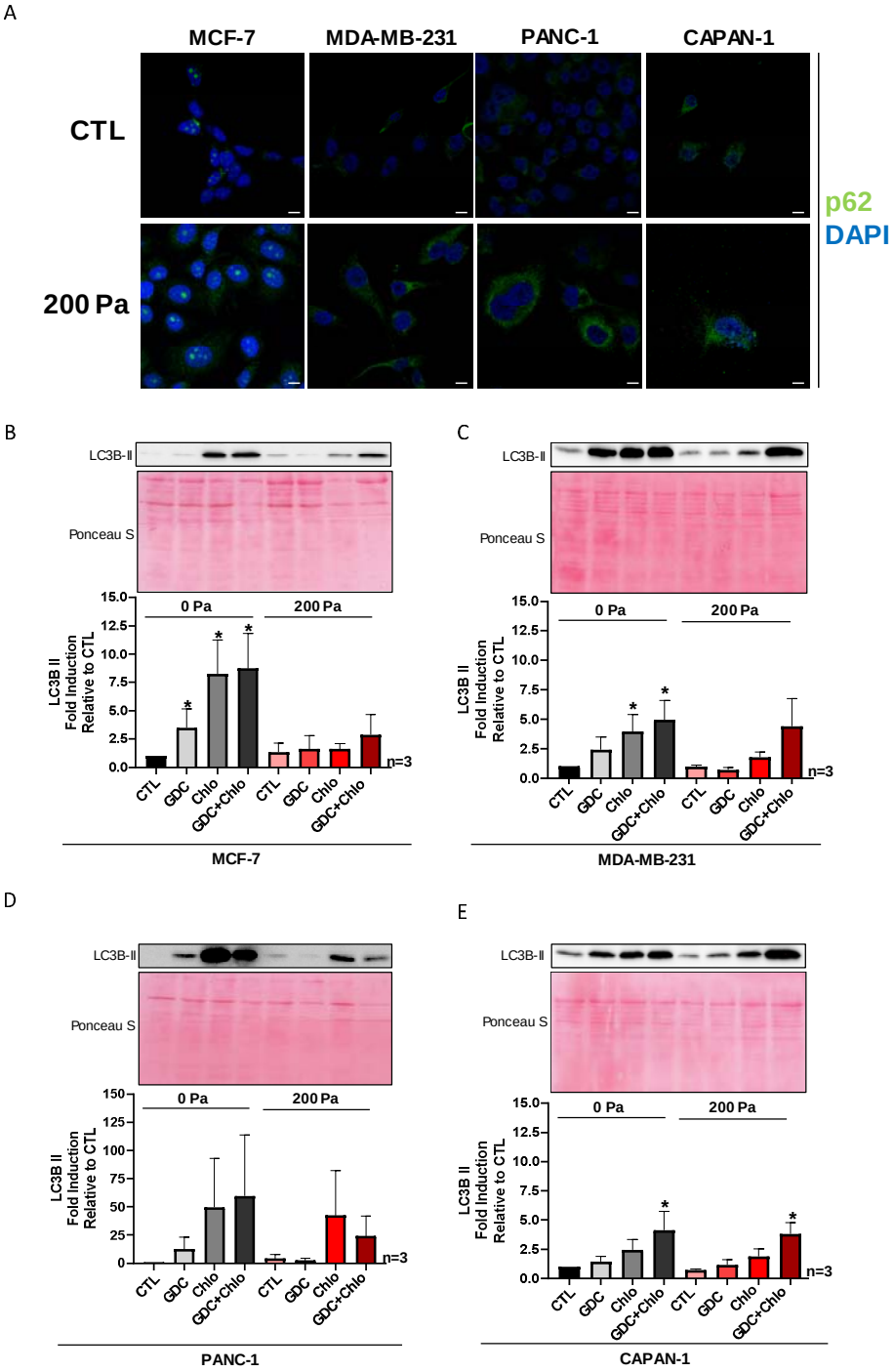

Figure 8. Autophagy flux in MCF-7/MDA-MB-231 breast and PANC-1/CAPAN-1 pancreatic cancer cells under 200 Pa compression. (**A**) p62/SQSTM1 staining in MCF-7, MDA-MB-231, PANC-1 and CAPAN-1 cells in uncompressed (CTL) and 200 Pa compressed conditions (200 Pa). Green fluorescence corresponds to p62/SQSTM1 and nuclear signal corresponds to DAPI. Scale bar correspond to 10µm. n=3. Representative western blots of LC3B II in MCF-7 (**B**), MDA-MB-231 (**C**), PANC-1 (**D**) and CAPAN-1 cells (**E**), in non-compressed (0 Pa) or compressed (200 Pa) conditions for 24h in control (CTL) pan-PI3K inhibitor (GDC-0941 (10µM)), chloroquine (Chlo (10 µM)),

pan-PI3K inhibitor + chloroquine (Chlo + GDC-0941 (10μM)). Ponceau S was used as loading control. LC3B II/ Ponceau S quantitative analyses were performed using ImageJ software and normalized to CTL 0 Pa. Results are presented as mean, +/- SEM, n≥3. *p-value<0.05.

3. Discussion

The impact of mechanical compressive forces on biological processes in cancer cells is still underexplored. Here, our major finding is that high intensity and static compression influences cell death in breast and pancreatic cancer cells. This effect can be accentuated by PI3K inhibition, opening avenues for compression in combination with PI3K inhibitors as a therapeutic intervention.

In terms of molecular mechanisms, the AKT activation by PI3K pathway has a well described important role in survival signaling. Activated AKT phosphorylates and inhibits the pro-apoptotic BCL-2 family members BAD, BAX, CASPASE-9, GSK-3, and FOXO1 which tightly regulates apoptosis (reviewed in [38]). The molecular mechanisms inducing cell death remains to be studied in further details. However, besides the pro-migratory [9] and proliferative [29] effects of compression-induced PI3K activation, we show in breast and pancreatic cancer cells that PI3K can also control cancer cell survival under compression.

Through our unbiased approach, we also identify another cell process, autophagy, as critically involved in determining the biological output of compression in cancer cells. Autophagy is a cellular process that allows the orderly degradation and recycling of cellular components, hence providing a self-promoted nutrient source benefiting cell homeostasis and survival [39]. Autophagy is a highly conserved catabolic process, participating to the balance of cell proliferation/death in tumor and the tumor microenvironment regulation. This process is highly regulated by PI3K-AKT-mTOR pathway in various tumors. We know that inhibition of PI3K-AKT-mTOR induces autophagy as part of a tumor growth suppressor role in early cancerogenesis [40, 41]. At cancer initiation, the autophagic flux participates to tissue homeostasis and helps to remove damaged cells. But, autophagy has a dual effect in cancer. In established cancers, autophagy promotes cancer cell survival and resistance to treatment. Autophagy is well known as a key therapeutic strategy for a variety of tumors including pancreatic cancer [42]. Interestingly, PI3K promotes autophagy in cancer cells with or without compression.

By comparing genes regulated by PI3Kα/PI3Kβ inhibitions, compressive stress and reactome PI3K-AKT signaling in cancer pathway lists of genes, we identified only *GABARAPL1* gene that overlap. This bioinformatics analysis was confirmed by our experimental data. GABARAP protein is modulated by compression in breast and pancreatic cancer cells and GABARAP protein level decreases or remains low in the two cell lines where PI3K inhibition further induces cell death under compression. GABARAP protein is cleaved by ATG4B protease before its conjugation to phospholipids. This modified lipidated form is localized on the surface of autophagosomes and lysosomes, participating in their formation. It is therefore involved in autophagy process (reviewed in [35]). The differential expression of GABARAP protein raises the possibility of a modula-

tion of autophagy flux (acceleration or blocking) and certainly of the stability of autophagosomes under compressive stress.

Finally, there are limited studies that link induction of autophagy with mechanical stress [21, 25]. In *Dictyostelium discoideum*, compression activates autophagy in a mTORC1 independent manner [24]. This mechanism, if confirmed in mammalian cells, could participate in cancer cell survival as well as resistance to chemotherapeutic treatments under compression.

Under increasing compression, gene/protein expression or phosphorylation status of PI3K-AKT and autophagy pathway members were significantly modulated. However, and surprisingly, "YAP/TAZ *via* Hippo" or "YAP/TAZ Non Hippo" pathway gene signatures and expression of YAP/TAZ-regulated genes were not significantly affected in breast and pancreatic cancer cells under unidirectional 2D compressive stress (Figure S2C). YAP/TAZ Hippo and non Hippo pathways are known as key regulators of mechanotransduction under tensile stress [43]. In compressive stress context, the implication of YAP/TAZ pathway was less investigated. It was assumed that this stress would induce the same signaling pathways as tensile stress. This assumption could have been prompted by the fact that some techniques used to induce compression could also promote tensile stress [44, 45]. In our study or in Kim *et al.* 2019 study [30], cells were compressed in 2D using pads without implementing additional tensile stress. We could argue that a threshold of tensile stress may be needed to permit the activation of YAP/TAZ. If our data seem to confirm those findings in the context of unidirectional compressive stress, differential cytoskeleton remodeling cannot be completely ruled out in our experimental conditions. The exact type of cytoskeleton remodeling under each mechanical stress may also be key to understand cell mechanotransduction processes, as cells adapt to the environmental stresses. Finally, PI3K signal is permissive for tensile stress control of YAP/TAZ and targeting of PI3K could be a novel strategy to hinder the potential YAP/TAZ oncogenic dependence [14].

Altogether, we show that breast and pancreatic cancers are sensitive to compression [9]. Further, ECM and desmoplasia may even be heterogeneously distributed in each PDAC tumor and influence the environment rigidity during progressive stages of the disease [46]. In addition to ECM-induced compressive stress, ECM also influences the tumor progression *via* epithelial-mesenchymal transition (EMT) and further contributes to resistance to chemotherapeutic agents [47]. Even if these high compressive stress situations occur mainly in breast cancer and PDAC [20, 48], our study provides an exploratory proof-of-concept of the impact of mechanical stresses on targetable oncogenic cell signaling. The efficiency of signal-targeted therapies combined with mechanotherapeutics should be investigated in a wider range of solid cancers.

Others have trialed therapeutic strategies that rely on decompression of solid tumor by reducing surrounding fibrosis and facilitating the accession of chemotherapeutic agents to the tumor [49-51]. They used monoclonal antibodies targeting either connective tissue growth factor (CTGF) (pamrevlumab, phase III), or extra-cellular matrix integrins (abituzumab, phase II), or the FAKs (defactinib or GSK2256098, phase II) for pancreatic

tumors or transforming growth factor β (LY3200882, phase I) in the case of certain solid tumors such as hepatocarcinomas [49]. These treatments reduce the surrounding fibrous tissue around the tumor and therefore may decrease compression forces induced by fibrosis. Some of these trials were stopped because they could accelerate the disease [51]. As compressive forces decrease proliferation of most cancer cells in *in vitro* 3D models and here even induces cell death, by reducing the surrounding fibrosis, those therapeutics could allow to increase the cancer cell proliferation, survival and promote tissue invasion and disease progression. These therapies should be considered in combination with conventional chemotherapies that can target newly proliferating cells freed from compressive context. It is even more important that compression of cancer cells without confinement increased cancer cell proliferative behaviour [8]. For these reasons, we are convinced that the balance between therapies reducing fibrosis and fibrosis-induced compression should be well mastered and individually adapted. Our findings also demonstrate that those mechanotherapeutics (modulating the mechanical environment in tumors) could also be used as a way to sensitize to oncogene targeted therapies [51].

4. Conclusion

In addition to the canonical pathways (YAP/TAZ and Piezo) associated with mechanical stresses, our study provides evidence for the role of PI3K-AKT pathway in compression-induced mechanotransduction, through class I PI3Ks. Moreover, other mechanisms inherent to compressive stress, such as cell death modulation and autophagy induction, may provide a proliferative advantage and sustain cell survival in compressive stress environment. Finally, oncogenic alterations are known to skew normal cell signaling. Associated to genetic alterations, environmental context such as compressive stress could also activate oncogenic pathways and induce novel tumoral vulnerabilities.

5. Material and Methods

PI3Kα genetic knockdown

MCF-7, MDA-MB-231, PANC-1 and CAPAN-1 cells were stably infected using lentiviral transduction containing p110α Sh-RNA or Scrambled-Sh-RNA into pLVTHM plasmid as described in [20]. Sh-RNA-p110α1 (F: 5′ CGCGTCCCCGCGAAATTCTCACACTATTATTTCAAGAGAATAATAGTGTGAGAATTTCGCTTTTTGGAAAT; R: 5′ CGATTTCCAAAAAGCGAAATTCTCACACTATTATTCTCTTGAAATAATAGTGTGAGAATTTCGCGGGGA); Sh-RNA-p110α2 (F: 5′ CGCGTCCCCGCACAATCCATGAACACATTTTCAAGGAAATGCTGTTCATGGATTGTGCTTTTTGGAAAT; R: 5′ CGATTTCCAAAAAGCACAATCCATGAACACATTTCTCTGAAAATGCTGTTCATGGATTGTGCGGGGA)

Scrambled-Sh-RNA (F: 5′ CGCGTCCCCTTCTAGAGATAGTCTGTACGTTTCAAGAGAACGTACAGACTATCTCTAGAATTTTTGGAAAT; R: 5′ CGATTTCCAAAAATTCTAGAGATAGTCTGTACGTTCTCTTGAAACGTACAGACTA

TCTCTAGAAGGGGA) and selected positively by cell sorted flow cytometry using GFP expression.

Cell culture

MCF-7 (ATCC; #CRL-3435), MDA-MB-231 (ATCC; # CRM-HTB-26), PANC-1 (ATCC; #CRL-1469) and CAPAN-1 cells (ATCC; #HTB-79) were cultured in Dulbecco's Modified Eagle Medium (GIBCO; #61965026) supplemented with 10% fetal bovine serum (Eurobio Scientific; #CVFSVF00-01), Penicillin-Streptomycin 50 U/mL and 50 µg/mL respectively (Sigma-Aldrich; #P0781), L-Glutamine 2 mM (Sigma-Aldrich; #G7513) and Plasmocin 25 µg/mL (InvivoGen; #ant-mpp) and maintained at 37°C in humidified atmosphere with 5% CO2. Cells were tested for their absence of mycoplasma infection prior use. MCF-7 contains a constitutive PI3Kα activation (*PIK3CA*^{E545K}) as compared to MDA-MB-231 cell line that harbors PI3Kα wild-type catalytic domain (*PIK3CA*^{WT}) [52]. Both pancreatic cancer cell lines present a constitutive PI3K activation [20].

2D compression

2x10^5 MCF-7, MDA-MB-231, PANC-1 or CAPAN-1 cells were plated in a 35 mm petri dish. MCF-7 and MDA-MB-231 were plated using Dulbecco's Modified Eagle Medium (GIBCO; #61965026) supplemented with indicated products in previous paragraph, however without phenol red. 24h after plating, a 2% low gelling temperature agarose pad (Sigma-Aldrich; #A0701-25G) in Phosphate Buffered Saline (PBS) containing 0.5 mM $MgCl_2$ and 0.9 mM $CaCl_2$ respectively (Sigma-Aldrich; #D8662) was deposited on cells. 2D compression was calibrated at 200 Pa per cell adjusting the weight with small metal plates on 2% agarose pad and calculated using the formula: P=(1/CN)*(1/CS)*m*g (with P=Pressure in Pa; CN=Cell number; CS=Cell surface in m^2; m=mass of the pad and metal plate in kg; g=gravitational force=9.80665 m/s-2). Controls were performed adding the volume of PBS 0.5 mM $MgCl_2$ and 0.9 mM $CaCl_2$ equivalent to the volume of the agarose pad. After 24h of compression, cells were harvested, and RNA/proteins were extracted.

Cell confluency assay

Cells were compressed following the protocol described above and/or treated with 10µM pan-PI3K inhibitor (GDC-0941; Axon Medchem) and/or Chloroquine (#C6628; Sigma-Aldrich) for 0h, 24h, 48h or 72h. After compression ± treatments, cells were rinsed with PBS (Eurobio Scientific, #CS1PBS 0101) and fixed for 15min using PBS containing 10% methanol and 10% acetic acid. Cells were stained for 15min using crystal violet (Sigma Aldrich; #HT90132). Images were performed using Chemidoc™ Imaging System (BioRad) and quantified using ImageJ software.

Protein extraction

Cells were rinsed with PBS and detached by scrapping in PBS. Cells were harvested through a 5min centrifugation at 3,000g and 4°C. Cells were resuspended in a lysis buffer containing 150 mM NaCl, 50 mM Tris, 1 mM EDTA, 1% Triton, 2 mM dithiothreitol, 2 mM Sodium fluoride, 4 mM Sodium Orthovanadate and supplemented with protease inhibitors (Complete protease inhibitors, Roche). After a 20min incubation on ice, a 10min centrifugation was performed at 12,000g and 4°C and the supernatant was collected. Protein concentration was measured using Bicinchoninic assay (BC Assay Protein Quantification Kit, #3082, Interchim).

Western Blot

20 µg of proteins were separated on a 10% polyacrylamide gel and transferred on nitrocellulose membranes (Amersham™ Protran®; #106000004) using Trans-Blot® Turbo™

(BioRad). Blocking was performed through a 1h incubation in 5% low fat milk in TBST. Membranes were incubated overnight at 4°C with primary antibodies in TBS-Tween 0.1%, 5% Bovine Serum Albumin as indicated in Supplementary Table 2. Then, membranes were rinsed three times with Tris-buffered saline 0,1% Tween (TBS-Tween 0.1%), incubated for 1h with secondary antibodies coupled to a horseradish peroxidase, in 1% low fat milk described in Supplementary Table 2. Membranes were next washed three times (1min, 5min and 10min) with TBS-Tween 0.1%. Proteins were detected through chemiluminescence (Clarity™ Western ECL Substrate; BioRad; #1705061) using Chemidoc™ Imaging System (BioRad) and quantified using ImageJ software. ≥3 independent replicates were performed for each protein analyzed.

Immunostaining

Cells were cultured on glass coverslips. After compression, cells were fixed with 4% PFA in PBS for 10min and then permeabilized with 0.1% Triton in PBS for 5min. Cells were blocked in blocking solution (1% BSA in PBS) for 30min. Samples were incubated with p62/SQSTM1 primary antibody (Supplementary Table 2) diluted into blocking solution overnight at 4°C. Cells were washed with PBS and then incubated with the Alexa Fluor® 488 secondary antibody diluted into blocking solution for 1h (Supplementary Table 3). Samples were washed with PBS and incubated with DAPI (Sigma; #D9542 0.1µg/ml) as nuclear counterstain, for 3min. Coverslips were mounted in Fluoromont-G (Invitrogen; # 00-4958-02).

Images were acquired with a Plan Aprochromat 63x ON 1.4 oil immersion objective using a Zeiss LSM780 confocal Microscope.

Annexin-V-FITC/Propidium Iodide (PI) assay

$2x10^5$ MCF-7, MDA-MB-231, PANC-1 or CAPAN-1 cells were plated in a 35 mm petri dish. 2D compression was calibrated at 200 Pa per cell adjusting the weight with small metal plates on 2% agarose pad according to 2D compression paragraph and were treated with 10 µM GDC-0941 (pan-PI3K inhibitor; Axon Medchem) for 24h.

After 24h of compression, cells were washed with fresh phosphate-buffered saline (PBS), trypsinized (supernatants were kept) and stained with a FITC-Annexin-V/PI apoptosis detection kit (BD Pharmigen #556547) according to the manufacturer's protocol. FITC-Annexin-V staining and PI incorporation were measured in cells with MACSQuant VYB Flow Cytometer and analyzed using FlowJo software.

RNA extraction

Cells were rinsed twice with PBS. Cell lysis was performed by scraping cells in 1 volume of TRIzol reagent (Ambion; #15596018), and incubating 5min on ice. Then, 1/5 volume of chloroform (Sigma Aldrich; #32211) was added to the mix Trizol/cell lysate. After 3min incubation at room temperature, cell lysate was centrifuged at 12,000g and 4°C, for 10min and the supernatant was collected. RNA was precipitated by adding 1 volume of isopropanol (Sigma Aldrich; #33539), incubated for 10min at room temperature and then centrifuged at 12,000g and 4°C for 10min. The RNA pellet was rinsed using 70° ethanol. After a 5min centrifugation at 7,500g and 4°C the supernatant was removed, the RNA pellet was air dried for 5min and resuspended in 30µL of RNAse free water. RNA concentration was measured using NanoDrop™ 2000 (ThermoFischer scientific).

Reverse transcription and quantitative PCR

cDNA synthesis was performed with iScript kit (BioRad; #1708891) according to the manufacturer protocol using C1000 Touch Thermal Cycler (BioRad) and the following conditions: annealing: 5min at 25°C, reverse transcription: 20min at 46°C, reverse tran-

scriptase inactivation: 1min at 95°C. cDNAs were diluted to a half in RNAse free water. Gene expression was quantified with the SsoFast EvaGreen supermix kit (BioRad, #1725204) using a thermocycler (StepOne™ #4376374; Software v2.2.2) with the following conditions: 20sec at 95°C, 40 denaturation cycles: 3sec at 95°C, annealing and elongation: 30sec at 60°C. β-actin was used as housekeeping gene. The primers used are described in Supplementary Table 1 and each amplicon was validated by sequencing. Gene expression quantification was performed using the Livak method: 2-(Delta Delta C(T)) [53]. Distinct RNA samples ≥4 were analyzed, each amplification was performed in technical duplicate.

Transcriptomic analysis

Differential expression analysis under compressive stress in MCF-7 and MDA-MB-231 cells were performed from data provided by Kim *et al.*, 2019 [30]. MCF-7 and MDA-MB-231 breast cancer cells were gradually compressed (0; 0.3 to 0.8; 1.5 to 4.0; 7.0 to 8.0 kPa) and gene expression was quantified using Agilent-039494 SurePrint G3 Human GE v2 8x60K Microarray 039381, data available at https://www.ncbi.nlm.nih.gov/geo/query/acc.cgi?acc=GSE133134. The two PI3Kα and PI3Kβ inhibition signatures were performed from differential expression analysis after PI3Kα inhibition with BYL-719 (1 μM for 16 to 48 hours) in MCF-7 breast cancer cells (https://www.ncbi.nlm.nih.gov/geo/query/acc.cgi?acc=GSE64033) [32] or PI3Kβ inhibition after AZD8186 treatment (100mg/kg twice daily for 5 days) in HCC70 cells (https://www.ebi.ac.uk/arrayexpress/experiments/E-MTAB-4656/) [33]. For compressive stress and PI3Kα and PI3Kβ inhibition signatures, differential expression analysis was performed using DESeq2 v1.26.0 [54] on R version 3.6.3 with adjusted p-value <0.05. All differential expression data are relative data from normalized transcript per million (TPM). P-values on graphs were calculated using t-test comparing no compression condition (0 kPa) to each compression condition ([0.3-0.8], [1.5-4.0] or [7.0-8.0] kPa). Enrichment analysis were performed using Gene Set Enrichment Analysis software (GSEA), p-value <0.05 and Fold Discovery Rate (FDR)<25%.

Statistical analysis

Comparisons between two experimental groups were performed using a paired two-tailed Student t-test. Comparisons between more than two experimental groups were performed using two-ways ANOVA. p-value<0.05 was considered significant. All analysis were performed using GraphPadPrism 9.3.1 software.

Supplementary Materials: The following are available online at www.mdpi.com/xxx/s1,

Figure S1. **PI3Kα (p110α) did not affect PI3Kβ (p110β) expression in pancreatic cancer cells**. Representative western blots of p110β after two different p110α knockdowns (sh-PI3Kα-1 and sh-PI3Kα-2) compared to control (sh-Scramble) in PANC-1 (**A**) and CAPAN-1 (**B**) cells. β-ACTIN was used as loading control. n=3.

Figure S2. ***In vitro* induction of apoptosis in MCF-7/MDA-MB-231 breast and PANC-1/CAPAN-1 pancreatic cancer cells after pharmaceutical inhibition of class I PI3K and 200 Pa compression**. After pan-PI3K inhibitor treatment and/or compression, cells were stained with a Annexin-V-FITC/PI apoptosis detection kit. Annexin-V-FITC staining and Propidium Iodide (PI) incorporation were measured in cells using a MACSQuant VYB Flow Cytometer and analyzed using FlowJo software. Early apoptotic cells correspond to the Annexin V positive and PI negative population. Late apoptotic and necrosis cells correspond to the Annexin V positive and PI positive population. Early and late apoptotic/necrosis cells populations were measured and quantified as cell

death in MCF-7 (**A**), MDA-MB-231 (**B**), PANC-1 (**C**) and CAPAN-1 (**D**) cells in control (CTL), 200 Pa compressed (200 Pa), pan-PI3K inhibitor (GDC-0941 (10μM)) and 200 Pa compressed with pan-PI3K inhibitor (200 Pa + GDC-0941 (10μM)) conditions. Most representative n of n=4.

Figure S3. **Housekeeping genes, PI3K-AKT, YAP/TAZ and autophagy pathways under increasing compressive stress in breast cancer cells**. MDA-MB-231 (PIK3CAwt; blue squares) and MCF-7 (PIK3CA^{E545K} mutated, black squares) breast cancer cells were gradually compressed (0 kPa; [0.3 to 0.8 kPa]; [1.5 to 4.0 kPa]; [7.0 to 8.0 kPa] respectively) and gene expression was quantified using Agilent microarray (Data available in https://www.ncbi.nlm.nih.gov/geo/query/acc.cgi?acc=GSE133134). Differentially expressed genes (p-value<0.05) were correlated. **A**. ACTINB (1 gene) and LAMINA1 (1 gene) and LAMIN gene class (12 genes) as housekeeping genes. **B**. Regulation of PI3K-AKT pathways and differential expression of class I PI3K members under increasing compression. **C**. Regulation of mechanoregulation and pathology of YAP/TAZ via HIPPO and non HIPPO mechanisms (45 genes) and autophagy (35 genes) pathways. ± SEM. *<0.05; **<0.01; ***<0.001.

Figure S4. **YAP/TAZ pathway under 200 Pa compressive stress in breast and pancreatic cancer cells**. A) MCF-7 and MDA-MB-231 breast cancer cells were compressed at 200 Pa for 24h and TEAD1, c-JUN, CCN1 and CCN2 mRNA expressions were quantified. β-ACTIN was used as housekeeping gene. B) PANC-1 and CAPAN-1 pancreatic cancer cells were 200 Pa compressed for 24h and TEAD1, c-JUN, CCN1 and CCN2 mRNA expressions were quantified. β-ACTIN was used as housekeeping gene. C) MCF-7 and MDA-MB-231 breast and PANC-1 and CAPAN-1 pancreatic cancer cells were 200 Pa compressed for 24h and p-YAP^{S127}/YAP protein expressions were quantified. β-ACTIN was used as loading control.

Author Contributions: Experimentation, analysis, visualisation and interpretation of data: MDL, CS, EB, NT, MC, RDA, BT and JGG. Supervision of students: MDL, JGG. Methodology: MDL, NT, RDA, BT, MD and JGG. Drafting of the manuscript: MDL, CS and JGG. Revising the manuscript: MDL, BT, MD and JGG. Conceptualization of funded project, obtained funding, project administration, project supervision, validation: MD and JGG.

Funding: Our work on this topic is funded by Fondation Toulouse Cancer Santé (Mecharesist), Inserm Plan Cancer (PressDiagTherapy; MECHAEVO), Inca PLBIO. CS and JGG obtained a Fondation Fonroga prize in this project.

Data Availability Statement: For this work, we utilized transcriptomic data from compressed breast cancer cells from Kim *et al.*, 2019 [30], from Gene Expression Omnibus GEO accession number: GSE133134. Our work correlates compression data to PI3Kα inhibition data from Bosch *et al.*, 2015 [32] GEO accession number: GSE64033) and PI3Kβ inhibition data from Lynch *et al.*, 2017 [33] ArrayExpress: ENA-ERP015852).

Acknowledgments: We thank our colleagues for their critical reading of the manuscript. CS is mentored by Ecole Normale Supérieure de Lyon, Université Claude Bernard Lyon 1, France.

Conflicts of Interest: The authors disclose no conflicts.

References

1. Lomakin, A. J.; Cattin, C. J.; Cuvelier, D.; Alraies, Z.; Molina, M.; Nader, G. P. F.; Srivastava, N.; Saez, P. J.; Garcia-Arcos, J. M.; Zhitnyak, I. Y.; Bhargava, A.; Driscoll, M. K.; Welf, E. S.; Fiolka, R.; Petrie, R. J.; De Silva, N. S.; Gonzalez-Granado, J. M.; Manel, N.; Lennon-Dumenil, A. M.; Muller, D. J.; Piel, M., The nucleus acts as a ruler tailoring cell responses to spatial constraints. *Science* **2020,** 370, (6514).
2. Northcott, J. M.; Dean, I. S.; Mouw, J. K.; Weaver, V. M., Feeling Stress: The Mechanics of Cancer Progression and Aggression. *Front Cell Dev Biol* **2018,** 6, 17.
3. Levental, K. R.; Yu, H.; Kass, L.; Lakins, J. N.; Egeblad, M.; Erler, J. T.; Fong, S. F.; Csiszar, K.; Giaccia, A.; Weninger, W.; Yamauchi, M.; Gasser, D. L.; Weaver, V. M., Matrix crosslinking forces tumor progression by enhancing integrin signaling. *Cell* **2009,** 139, (5), 891-906.
4. Li, Y.; Chen, M.; Hu, J.; Sheng, R.; Lin, Q.; He, X.; Guo, M., Volumetric Compression Induces Intracellular Crowding to Control Intestinal Organoid Growth via Wnt/beta-Catenin Signaling. *Cell Stem Cell* **2021,** 28, (1), 63-78 e7.
5. Provenzano, P. P.; Cuevas, C.; Chang, A. E.; Goel, V. K.; Von Hoff, D. D.; Hingorani, S. R., Enzymatic targeting of the stroma ablates physical barriers to treatment of pancreatic ductal adenocarcinoma. *Cancer Cell* **2012,** 21, (3), 418-29.
6. Therville, N.; Arcucci, S.; Vertut, A.; Ramos-Delgado, F.; Da Mota, D. F.; Dufresne, M.; Basset, C.; Guillermet-Guibert, J., Experimental pancreatic cancer develops in soft pancreas: novel leads for an individualized diagnosis by ultrafast elasticity imaging. *Theranostics* **2019,** 9, (22), 6369-6379.
7. Delarue, M.; Montel, F.; Vignjevic, D.; Prost, J.; Joanny, J. F.; Cappello, G., Compressive stress inhibits proliferation in tumor spheroids through a volume limitation. *Biophys J* **2014,** 107, (8), 1821-1828.
8. Mary, G.; Malgras, B.; Perez, J. E.; Nagle, I.; Luciani, N.; Pimpie, C.; Asnacios, A.; Pocard, M.; Reffay, M.; Wilhelm, C., Magnetic Compression of Tumor Spheroids Increases Cell Proliferation In Vitro and Cancer Progression In Vivo. *Cancers (Basel)* **2022,** 14, (2).
9. Kalli, M.; Minia, A.; Pliaka, V.; Fotis, C.; Alexopoulos, L. G.; Stylianopoulos, T., Solid stress-induced migration is mediated by GDF15 through Akt pathway activation in pancreatic cancer cells. *Sci Rep* **2019,** 9, (1), 978.
10. Kalli, M.; Li, R.; Mills, G. B.; Stylianopoulos, T.; Zervantonakis, I. K., Mechanical Stress Signaling in Pancreatic Cancer Cells Triggers p38 MAPK- and JNK-Dependent Cytoskeleton Remodeling and Promotes Cell Migration via Rac1/cdc42/Myosin II. *Mol Cancer Res* **2021**.
11. Rizzuti, I. F.; Mascheroni, P.; Arcucci, S.; Ben-Meriem, Z.; Prunet, A.; Barentin, C.; Riviere, C.; Delanoe-Ayari, H.; Hatzikirou, H.; Guillermet-Guibert, J.; Delarue, M., Mechanical Control of Cell Proliferation Increases Resistance to Chemotherapeutic Agents. *Phys Rev Lett* **2020,** 125, (12), 128103.
12. Cobbaut, M.; Karagil, S.; Bruno, L.; Diaz de la Loza, M. D. C.; Mackenzie, F. E.; Stolinski, M.; Elbediwy, A., Dysfunctional Mechanotransduction through the YAP/TAZ/Hippo Pathway as a Feature of Chronic Disease. *Cells* **2020,** 9, (1).
13. Piccolo, S.; Dupont, S.; Cordenonsi, M., The biology of YAP/TAZ: hippo signaling and beyond. *Physiol Rev* **2014,** 94, (4), 1287-312.
14. Di-Luoffo, M.; Ben-Meriem, Z.; Lefebvre, P.; Delarue, M.; Guillermet-Guibert, J., PI3K functions as a hub in mechanotransduction. *Trends Biochem Sci* **2021**.
15. Zhao, Y.; Montminy, T.; Azad, T.; Lightbody, E.; Hao, Y.; SenGupta, S.; Asselin, E.; Nicol, C.; Yang, X., PI3K Positively Regulates YAP and TAZ in Mammary Tumorigenesis Through Multiple Signaling Pathways. *Mol Cancer Res* **2018,** 16, (6), 1046-1058.
16. Borreguero-Munoz, N.; Fletcher, G. C.; Aguilar-Aragon, M.; Elbediwy, A.; Vincent-Mistiaen, Z. I.; Thompson, B. J., The Hippo pathway integrates PI3K-Akt signals with mechanical and polarity cues to control tissue growth. *PLoS Biol* **2019,** 17, (10), e3000509.

17. Vanhaesebroeck, B.; Guillermet-Guibert, J.; Graupera, M.; Bilanges, B., The emerging mechanisms of isoform-specific PI3K signalling. *Nat Rev Mol Cell Biol* **2010,** 11, (5), 329-41.
18. Arcucci, S.; Ramos-Delgado, F.; Cayron, C.; Therville, N.; Gratacap, M. P.; Basset, C.; Thibault, B.; Guillermet-Guibert, J., Organismal roles for the PI3Kalpha and beta isoforms: their specificity, redundancy or cooperation is context-dependent. *Biochem J* **2021,** 478, (6), 1199-1225.
19. Pons-Tostivint, E.; Thibault, B.; Guillermet-Guibert, J., Targeting PI3K Signaling in Combination Cancer Therapy. *Trends Cancer* **2017,** 3, (6), 454-469.
20. Thibault, B.; Ramos-Delgado, F.; Pons-Tostivint, E.; Therville, N.; Cintas, C.; Arcucci, S.; Cassant-Sourdy, S.; Reyes-Castellanos, G.; Tosolini, M.; Villard, A. V.; Cayron, C.; Baer, R.; Bertrand-Michel, J.; Pagan, D.; Ferreira Da Mota, D.; Yan, H.; Falcomata, C.; Muscari, F.; Bournet, B.; Delord, J. P.; Aksoy, E.; Carrier, A.; Cordelier, P.; Saur, D.; Basset, C.; Guillermet-Guibert, J., Pancreatic cancer intrinsic PI3Kalpha activity accelerates metastasis and rewires macrophage component. *EMBO Mol Med* **2021,** 13, (7), e13502.
21. Xu, Z.; Han, X.; Ou, D.; Liu, T.; Li, Z.; Jiang, G.; Liu, J.; Zhang, J., Targeting PI3K/AKT/mTOR-mediated autophagy for tumor therapy. *Appl Microbiol Biotechnol* **2020,** 104, (2), 575-587.
22. Heras-Sandoval, D.; Perez-Rojas, J. M.; Hernandez-Damian, J.; Pedraza-Chaverri, J., The role of PI3K/AKT/mTOR pathway in the modulation of autophagy and the clearance of protein aggregates in neurodegeneration. *Cell Signal* **2014,** 26, (12), 2694-701.
23. King, J. S., Mechanical stress meets autophagy: potential implications for physiology and pathology. *Trends Mol Med* **2012,** 18, (10), 583-8.
24. King, J. S.; Veltman, D. M.; Insall, R. H., The induction of autophagy by mechanical stress. *Autophagy* **2011,** 7, (12), 1490-9.
25. Claude-Taupin, A.; Codogno, P.; Dupont, N., Links between autophagy and tissue mechanics. *J Cell Sci* **2021,** 134, (17).
26. Pascual, J.; Turner, N. C., Targeting the PI3-kinase pathway in triple-negative breast cancer. *Ann Oncol* **2019,** 30, (7), 1051-1060.
27. Ellis, H.; Ma, C. X., PI3K Inhibitors in Breast Cancer Therapy. *Curr Oncol Rep* **2019,** 21, (12), 110.
28. Stylianopoulos, T., The Solid Mechanics of Cancer and Strategies for Improved Therapy. *J Biomech Eng* **2017,** 139, (2).
29. Nam, S.; Gupta, V. K.; Lee, H. P.; Lee, J. Y.; Wisdom, K. M.; Varma, S.; Flaum, E. M.; Davis, C.; West, R. B.; Chaudhuri, O., Cell cycle progression in confining microenvironments is regulated by a growth-responsive TRPV4-PI3K/Akt-p27(Kip1) signaling axis. *Sci Adv* **2019,** 5, (8), eaaw6171.
30. Kim, B. G.; Sung, J. S.; Jang, Y.; Cha, Y. J.; Kang, S.; Han, H. H.; Lee, J. H.; Cho, N. H., Compression-induced expression of glycolysis genes in CAFs correlates with EMT and angiogenesis gene expression in breast cancer. *Commun Biol* **2019,** 2, 313.
31. Cairns, R. A.; Harris, I. S.; Mak, T. W., Regulation of cancer cell metabolism. *Nat Rev Cancer* **2011,** 11, (2), 85-95.
32. Bosch, A.; Li, Z.; Bergamaschi, A.; Ellis, H.; Toska, E.; Prat, A.; Tao, J. J.; Spratt, D. E.; Viola-Villegas, N. T.; Castel, P.; Minuesa, G.; Morse, N.; Rodon, J.; Ibrahim, Y.; Cortes, J.; Perez-Garcia, J.; Galvan, P.; Grueso, J.; Guzman, M.; Katzenellenbogen, J. A.; Kharas, M.; Lewis, J. S.; Dickler, M.; Serra, V.; Rosen, N.; Chandarlapaty, S.; Scaltriti, M.; Baselga, J., PI3K inhibition results in enhanced estrogen receptor function and dependence in hormone receptor-positive breast cancer. *Sci Transl Med* **2015,** 7, (283), 283ra51.
33. Lynch, J. T.; Polanska, U. M.; Delpuech, O.; Hancox, U.; Trinidad, A. G.; Michopoulos, F.; Lenaghan, C.; McEwen, R.; Bradford, J.; Polanski, R.; Ellston, R.; Avivar-Valderas, A.; Pilling, J.; Staniszewska, A.; Cumberbatch, M.; Critchlow, S. E.; Cruzalegui, F.; Barry, S. T., Inhibiting PI3Kbeta with AZD8186 Regulates Key Metabolic Pathways in PTEN-Null Tumors. *Clin Cancer Res* **2017,** 23, (24), 7584-7595.
34. Chalhoub, N.; Baker, S. J., PTEN and the PI3-kinase pathway in cancer. *Annu Rev Pathol* **2009,** 4, 127-50.

35. Le Grand, J. N.; Chakrama, F. Z.; Seguin-Py, S.; Fraichard, A.; Delage-Mourroux, R.; Jouvenot, M.; Boyer-Guittaut, M., GABARAPL1 (GEC1): original or copycat? *Autophagy* **2011,** 7, (10), 1098-107.
36. Bjorkoy, G.; Lamark, T.; Pankiv, S.; Overvatn, A.; Brech, A.; Johansen, T., Monitoring autophagic degradation of p62/SQSTM1. *Methods Enzymol* **2009,** 452, 181-97.
37. Mauthe, M.; Orhon, I.; Rocchi, C.; Zhou, X.; Luhr, M.; Hijlkema, K. J.; Coppes, R. P.; Engedal, N.; Mari, M.; Reggiori, F., Chloroquine inhibits autophagic flux by decreasing autophagosome-lysosome fusion. *Autophagy* **2018,** 14, (8), 1435-1455.
38. Miricescu, D.; Totan, A.; Stanescu, S., II; Badoiu, S. C.; Stefani, C.; Greabu, M., PI3K/AKT/mTOR Signaling Pathway in Breast Cancer: From Molecular Landscape to Clinical Aspects. *Int J Mol Sci* **2020,** 22, (1).
39. Poillet-Perez, L.; White, E., Role of tumor and host autophagy in cancer metabolism. *Genes Dev* **2019,** 33, (11-12), 610-619.
40. Cui, L. H.; Li, C. X.; Zhuo, Y. Z.; Yang, L.; Cui, N. Q.; Zhang, S. K., Saikosaponin d ameliorates pancreatic fibrosis by inhibiting autophagy of pancreatic stellate cells via PI3K/Akt/mTOR pathway. *Chem Biol Interact* **2019,** 300, 18-26.
41. Yang, J.; Pi, C.; Wang, G., Inhibition of PI3K/Akt/mTOR pathway by apigenin induces apoptosis and autophagy in hepatocellular carcinoma cells. *Biomed Pharmacother* **2018,** 103, 699-707.
42. Bryant, K. L.; Stalnecker, C. A.; Zeitouni, D.; Klomp, J. E.; Peng, S.; Tikunov, A. P.; Gunda, V.; Pierobon, M.; Waters, A. M.; George, S. D.; Tomar, G.; Papke, B.; Hobbs, G. A.; Yan, L.; Hayes, T. K.; Diehl, J. N.; Goode, G. D.; Chaika, N. V.; Wang, Y.; Zhang, G. F.; Witkiewicz, A. K.; Knudsen, E. S.; Petricoin, E. F., 3rd; Singh, P. K.; Macdonald, J. M.; Tran, N. L.; Lyssiotis, C. A.; Ying, H.; Kimmelman, A. C.; Cox, A. D.; Der, C. J., Combination of ERK and autophagy inhibition as a treatment approach for pancreatic cancer. *Nat Med* **2019,** 25, (4), 628-640.
43. Totaro, A.; Panciera, T.; Piccolo, S., YAP/TAZ upstream signals and downstream responses. *Nat Cell Biol* **2018,** 20, (8), 888-899.
44. Kalli, M.; Voutouri, C.; Minia, A.; Pliaka, V.; Fotis, C.; Alexopoulos, L. G.; Stylianopoulos, T., Mechanical Compression Regulates Brain Cancer Cell Migration Through MEK1/Erk1 Pathway Activation and GDF15 Expression. *Front Oncol* **2019,** 9, 992.
45. Chen, Y.; Li, Z.; Ju, L. A., Tensile and compressive force regulation on cell mechanosensing. *Biophys Rev* **2019,** 11, (3), 311-318.
46. Provenzano, P. P.; Hingorani, S. R., Hyaluronan, fluid pressure, and stromal resistance in pancreas cancer. *Br J Cancer* **2013,** 108, (1), 1-8.
47. Rice, A. J.; Cortes, E.; Lachowski, D.; Cheung, B. C. H.; Karim, S. A.; Morton, J. P.; Del Rio Hernandez, A., Matrix stiffness induces epithelial-mesenchymal transition and promotes chemoresistance in pancreatic cancer cells. *Oncogenesis* **2017,** 6, (7), e352.
48. Verret, B.; Cortes, J.; Bachelot, T.; Andre, F.; Arnedos, M., Efficacy of PI3K inhibitors in advanced breast cancer. *Ann Oncol* **2019,** 30, (Suppl_10), x12-x20.
49. Sheridan, C., Pancreatic cancer provides testbed for first mechanotherapeutics. *Nat Biotechnol* **2019,** 37, (8), 829-831.
50. Lampi, M. C.; Reinhart-King, C. A., Targeting extracellular matrix stiffness to attenuate disease: From molecular mechanisms to clinical trials. *Sci Transl Med* **2018,** 10, (422).
51. Mohammadi, H.; Sahai, E., Mechanisms and impact of altered tumour mechanics. *Nat Cell Biol* **2018,** 20, (7), 766-774.
52. Dunn, S.; Lombardi, O.; Lukoszek, R.; Cowling, V. H., Oncogenic PIK3CA mutations increase dependency on the mRNA cap methyltransferase, RNMT, in breast cancer cells. *Open Biol* **2019,** 9, (4), 190052.
53. Livak, K. J.; Schmittgen, T. D., Analysis of relative gene expression data using real-time quantitative PCR and the 2(-Delta Delta C(T)) Method. *Methods* **2001,** 25, (4), 402-8.
54. Anders, S.; Huber, W., Differential expression analysis for sequence count data. *Genome Biol* **2010,** 11, (10), R106.